Proceedings of the ASME 2015 Dynamic Systems and Control Conference
DSCC2015
October 28-30, 2015, Columbus, Ohio, USA

DSCC2015-9774

INSTRUMENTED WALKWAY FOR ESTIMATION OF THE ANKLE IMPEDANCE IN DORSIFLEXION-PLANTARFLEXION AND INVERSION-EVERSION DURING STANDING AND WALKING

Evandro M. Ficanha
Department of Mechanical Engineering-Engineering Mechanics
Michigan Technological University
Houghton, Michigan 49931
emficanh@mtu.edu

Guilherme Ribeiro
Department of Mechanical Engineering-Engineering Mechanics
Michigan Technological University
Houghton, Michigan 49931
garamizo@mtu.edu

Mohammad Rastgaar Aagaah
Department of Mechanical Engineering-Engineering Mechanics
Michigan Technological University
Houghton, Michigan 49931
rastgaar@mtu.edu

ABSTRACT

This paper describes in detail the fabrication of an instrumented walkway for estimation of the ankle mechanical impedance in both dorsiflexion-plantarflexion (DP) and in inversion-eversion (IE) directions during walking in arbitrary directions and standing. The platform consists of two linear actuators, each capable of generating ±351.3 N peak force that are mechanically coupled to a force plate using Bowden cables. The applied forces cause the force plate to rotate in two degrees of freedom (DOF) and transfer torques to the human ankle to generate DP and IE rotations. The relative rotational motion of the foot with respect to the shin is recorded using a motion capture camera system while the forces applied to the foot are measured with the force plate, from which the torques applied to the ankle are calculated. The analytical methods required for the estimation of the ankle torques, rotations, and impedances are presented. To validate the system, a mockup with known stiffness was used, and it was shown that the developed system was capable of properly estimating the stiffness of the mockup in two DOF with less than 5% error. Also, a preliminary experiment with a human subject in standing position was performed, and the estimated quasi-static impedance of the ankle was estimated at 319 Nm/rad in DP and 119 Nm/rad in IE.

INTRODUCTION

The human ankle plays a major role in locomotion. It supports the weight of the whole body while rotating in all anatomical planes and accommodating environment stimulus. To accomplish such complex tasks, the ankle's mechanical impedance is continuously modulated. The impedance of a mechanical system correlates the resultant motion due to an input force, and it is a function of the system stiffness, damping, and inertia. Powered ankle-foot prostheses may benefit from mimicking the human ankle's mechanical impedance during walking resulting in similar mechanical characteristics as the limbs of an unimpaired human. The quasi-static impedance of the ankle in sagittal plane has been used in the control of lower extremity powered prostheses [1-3].

The mechanical impedance of the ankle in both DP and IE has been studied in non-load bearing conditions for dynamic impedance [4, 5], and in quasi-static impedance [6-8]. However, non-load bearing conditions may not fully represent the function of the ankle during standing and walking. Shamaei et al. developed a model to estimate the quasi-static impedance and work of the ankle as a function of the gait speed, ankle excursion, and the subjects' height and weight. [9]. Recently, two different studies have reported the estimation of the mechanical impedance of the human ankle during walking. Rouse et al. developed a mechatronic platform to apply perturbations to the ankle in a single DOF (sagittal plane) during the stance phase of walking. The perturbations were applied at four distinct points in the range of 13% to 63% of the stance phase. This study showed great variability in the ankle stiffness and damping in the studied range of the stance phase [10]. However this study was conducted in one DOF in DP direction. Lee et al. used a wearable rehabilitation robot to apply continuous random perturbations to the ankle as a subject walked on a treadmill to estimate the mechanical impedance during the swing and stance phases of the gait [11]. Although wearing the perturbation robot during the test allowed for the estimation of the ankle impedance during the swing phase, it requires the user to carry the weight of the robot that may alter the walking dynamics. Also, the amount of power generated by the wearable robot is limited, and the subject was constrained to walk on a treadmill.

This paper describes the design and fabrication of an instrumented walkway capable of continuously applying pseudo-random perturbation to the ankle in two DOF during the entire stance phase of the gait. It has the benefit of having a powered platform so the user does not need to wear or carry any measurement device or actuation system other than reflective markers used to record the ankle kinematics with a motion capture camera system. The instrumented walkway was design for the measurement of the ankle mechanical impedance during walking in arbitrary directions, including sidestep cutting and turning. This paper describes in detail the construction of the instrumented walkway and preliminary experiments with a mockup with known stiffness to validate the capability of the system to estimate the impedance of a dynamic system using a correlation-based least-squares method. Also, preliminary results on the estimation of the impedance of a human subject's ankle during standing is presented. One male subjects with no self-reported neuromuscular and biomechanical disorders was participated in the experiments. The subject gave written consents, which was approved by the Michigan Tech's Institutional Review Board.

INSTRUMENTED PERTURBATION PLATFORM

The perturbation platform (Fig. 1) consists of two independent modules; force plate and actuation modules, connected by four Bowden cables. This low profile design allows for installing the force plate module in an instrumented walkway by placing the actuation systems on the side. The actuation module contains all the power electronics and motors and the force plate module contains a 2-DOF platform that uses the power transferred through the Bowden cables to rotate a force plate in two DOFs.

The actuation module (Fig. 2) is driven by two linear voice coil actuators (A) (Moticont® GVCM-095-089-01). The motors are capable of producing ±351.3 N of force at 10% duty cycle or ±111.2 N continuously and have a 63.5 mm stroke length. The voice coils are powered by a pair of digital servo drivers (B) (Moticont® 510-03). The servo drivers run on an open loop current control and receive signals from a DAC board (C) connected to a computer. Each motor is connected to two Bowden cables (D), one on each end of the motor. This way, each motor can pull on one cable while releasing the tension on the opposite side. The Bowden cable housing are attached to two flexible carbon fiber plates (E) which are preloaded to assure the cables are always under tension. The flexible carbon fiber plates are mounted to a rail (F), allowing for easy adjustment of the neutral position of the motors with respect to the force plate and preloading of the tension on the cables. Proper cable pre-load is essential as excessive load increases the friction inside the Bowden cables reducing the available power to the force plate module. Insufficient pre-load may result in cable slack during the experiments when the motors remove the tension on the cables. For maximum efficiency of the Bowden cables, the cable pre-load was increased sufficiently to remove all cable slack during the experiments.

The force plate module with the force plate removed can be seen in Fig. 3. The force plate (G) (Kistler® 9260AA3) can be easily connected and disconnected from the frame (H) allowing it to be used elsewhere. The force plate feet (I) are inserted inside the sleeves (J) with a tight fit with no gap between each foot and its respective sleeve. This is assured by rubber O-rings around each foot. In the center of the top frame (H) a universal joint (K) constrains the frame and the force plate from any

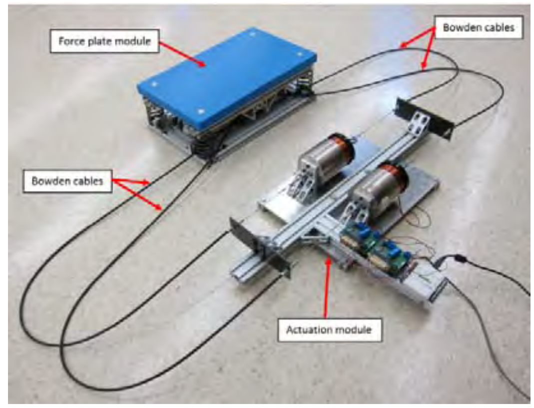

Fig. 1: Perturbation platform and its main modules.

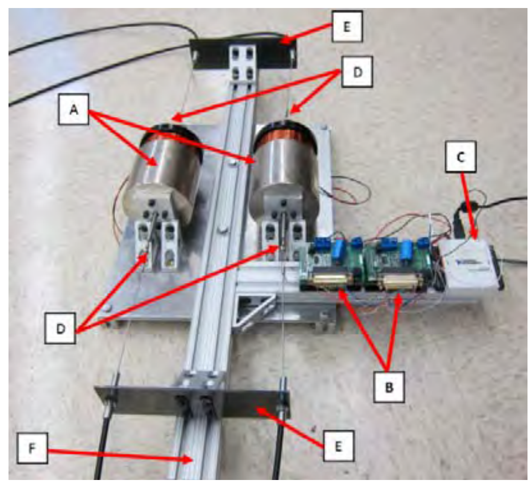

Fig 2. Actuation module and its main components.

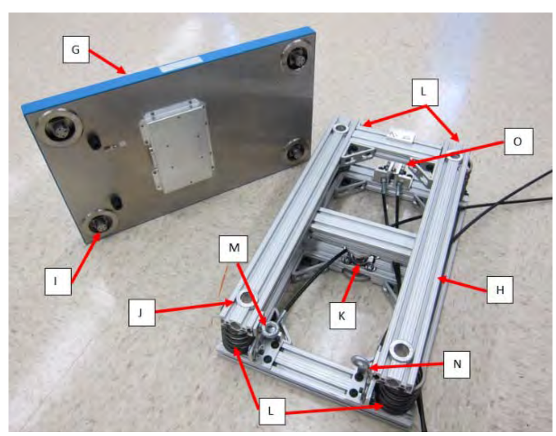

Fig. 3: Force plate module with the force plate removed.

translation and from rotating about the vertical axis. The universal joint contains low friction needle bearings rated for load bearing. The rotations of the force plate impose DP and IE rotations when the foot is on top of the force plate. Springs (L) are attached at each corner of the frame (H). The springs are rated at 12 kN/m and are preloaded 0.025 m. The resultant rotational stiffness is 270 Nm/deg in DP and 150 Nm/deg in IE. The universal joint is necessary to hold the user's weight while constraining the force plate from sliding in the horizontal plane. The springs are necessary to maintain the force plate rotational position near centered with the top surface of the force plate horizontal, allowing a subject to walk on top of it and resisting the torque generated by the ankle while the motors apply perturbations. The Bowden cables are attached to three points in the lower part of frame H at points M, N, and O. After the cables exit the Bowden cable housing, the cables turn 90° upwards using pulleys and connect directly to the upper part of frame H.

The perturbation platform was incorporated into a walkway (Fig. 4). The walkway has the same height as the perturbation platform and measures 6 m in length by 1.83 m in width. The walkway has been designed for gait analysis and is made of solid wood to avoid undesired vibrations that a hollow walkway may generate. The instrumented walkway uses a motion capture camera system consisted of eight Prime 17W Optitrack®. The cameras are mounted in a square formation covering a volume of about 16 cubic meters and an area of 12 square meters. The cameras emit infrared light and capture the reflected light from the reflector markers placed on the participants.

EVALUATION USING A MOCKUP

An experiment was performed to validate the capability of the instrumented walkway to estimate the impedance of a known system. A mockup (Fig. 5) consisted of a wooden frame was rigidly attached to the walkway and two springs were mounted at known distances from both axes of rotation of the force plate. Two infrared markers were installed on the mockup above the springs and two markers were installed at the force plate next to the springs. The compression of each spring was estimated as the change in the vertical distance between the markers on the mockup and the markers on the force plate. This subtraction of the wooden frame movement assures that the stiffness of the wooden frame does not interfere with the spring's impedance estimation. The experiment was conducted as shown in Fig. 5 to estimate torques applied in DP. The springs are located in the farthest point from the center of rotation of the force plate in the longitudinal direction, so the torques necessary to compress the springs are similar to the torques required to rotate the foot in DP. To simulate the torques in IE, the mockup was rotated 90° counterclockwise, so the springs are located in the farthest point of the force plate from the center of rotation in the lateral direction. The expected stiffness based on the stiffness of the springs and the moment arm between the springs and the center of rotation of the force plate were estimated to be 1154 Nm/rad and 313 Nm/rad for DP and IE, respectively. Uncorrelated pseudo random current inputs were applied to each of the actuators to apply the torque perturbations to the mockup causing the spring to compress. The bandwidth of the input signals was set to 30 Hz and the experiment lasted 60 seconds. The camera system and the force plate were set to record at motion and forces at 300 Hz.

The measured variables were the compression displacements X_L and X_R of the springs on the left and right of the force plate respectively and the commanded forces F_z perpendicular to the force plate surface. The resultant torque (τ) and angle (θ) were estimated based on the compression displacements X_L and X_R and the distance from the springs to the axes of rotation of the force plate (D) that is 0.21 m in DP and 0.11 m in IE.

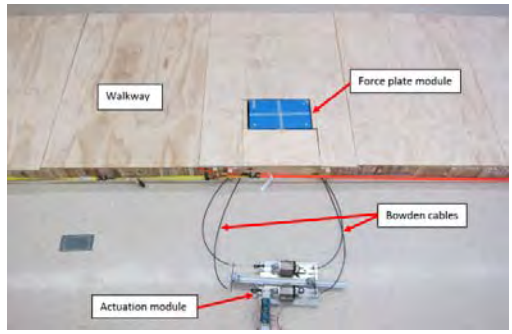

Fig. 4: Instrumented walkway and its main components (cameras are not shown).

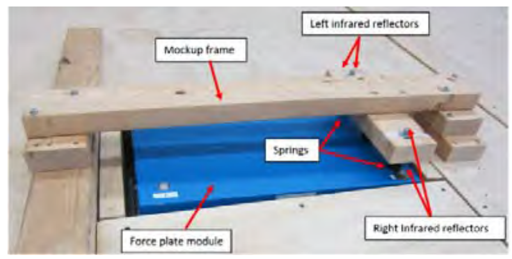

Fig. 5: Mockup configured for impedance representation of DP torques.

$$\tau = D \times F_z \tag{1}$$

$$\theta = \frac{1}{D} \times \frac{X_R + X_L}{2} \tag{2}$$

Current inputs to the actuators generated forces that resulted in the compression of the springs. A proper description of this system is a mechanical admittance (force input, motion output). Assuming linear dynamics, the admittance $Y(f)$ defined as a transfer function that relates torque inputs to displacement outputs:

$$\theta(f) = Y(f)\tau(f) \tag{3}$$

and its inverse is the mechanical impedance $Z(f)$.

$$Z(f) = Y^{-1}(f) \tag{4}$$

Which can be described as a transfer function relating input angles to output torques:

$$\tau(f) = Z(f)\theta(f) \tag{5}$$

Equation 5 implies that the mechanical impedance of the system under test is:

$$Z(f) = \frac{\tau(f)}{\theta(f)} \tag{6}$$

Where the impedance functions τ and θ are determined from the experimental measurements. Although the system naturally behaves as a mechanical admittance, expressing it as a mechanical impedance simplifies separating the force plate dynamics from the mockup dynamics, or in the case of human tests, the human ankle dynamics. The force plate and mockup share the same motion, consequently the torque exerted by the actuator is the sum of the torques required to move the force plate and mockup; the output mechanical impedance of the force plate adds to the mockup impedance. The mockup's impedance is obtained by subtracting the estimated impedance of the force plate alone from the estimated impedance of the force plate and mockup together as follows:

$$\mathbf{Z}|_{mockup} = \mathbf{Z}|_{mockup\ +\ force\ \ plate} - \mathbf{Z}|_{force\ \ plate} \qquad (7)$$

where the $Z|_{force\ plate}$ was estimated with an experiment with the springs removed from the mockup.

Frequency domain stochastic methods were used to estimate the mechanical impedance. Sixty five seconds of data were sampled at 300 Hz yielding 18,000 samples after the first 5 seconds of data were removed. The MATLAB®'s *tfestimate* function was used to estimate the transfer function relating input angles to output torques. Periodic Hamming windows with a length of 512 samples and 50% overlap (256 samples) were used with a Fast Fourier Transform (FFT) length of 1024 samples. In addition, the coherence function was estimated to measure the linear relationship between the input and output using MATLAB®'s *mscohere* function with similar window length, overlap, and FFT lengths. The impedance plots of these experiments can be seen in Fig. 6. The estimated stiffness (quasi-static impedance) of the mockup was measured to be 1100 Nm/rad in DP and 298 Nm/rad in IE at 1 Hz. These values were 4.7% and 5.0% less than the calculated value based on the measured spring stiffness and the geometry of the mockup. The coherence values were always above 0.8 in the frequency range of interest, showing a desirable linear relationship between angles and torques.

HUMAN ANKLE IMPEDANCE ESTIMATION DURING STANDING

The ankle angles and the disturbance torques applied to the ankle are necessary to estimate the impedance of the human ankle. To estimate the ankle angles (the angles of the foot with respect to the shin) polycarbonate plastic rigid frames with reflective markers developed by the camera system manufacturer were placed on the foot and the shin of the human subject, as described in [12]. The force plate reaction forces and the moment arms between the ankle center of rotation and the foot center of pressure were required to calculate the torques applied to the ankle. The foot center of pressure was on the surface of the force plate in the force plate Coordinate System (CS) and was estimated from the force plate readings. To estimate the center of pressure in the foot CS, four reflective markers were installed on the force plate (one on each corner of the top surface of the force plate), and the rotations of the force plate were recorded. The center of pressure was transformed from the force plate CS to the foot CS using the measured rotations of the foot and force plate in the global CS. The instantaneous ankle center of rotation was estimated as described in [12]. Next, the ankle torques were calculated based on the moment arms that are the components of the vector from the ankle center of rotation to the foot center of pressure in the foot CS and the force plate reaction forces transformed from the force plate CS to the foot CS.

The sampling rates of the force plate and camera system were set to 300 Hz and the actuators received uncorrelated

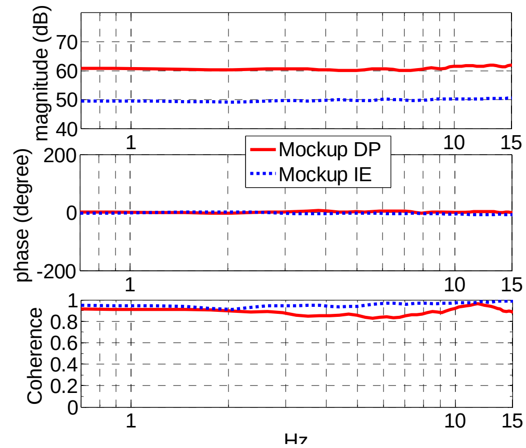

Fig. 6: Magnitude, phase, and coherence plots of the mockup's mechanical impedance in DP and IE.

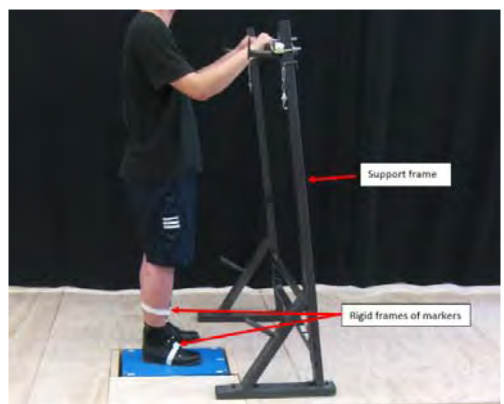

Fig. 7: A human subject standing on the perturbation platform during impedance estimation of the human ankle.

pseudo random current inputs to apply the perturbations to the ankle. The frequency of interests is 0 to 15 Hz, as 99% of the gait power (as a percent of the total power spectrum content in the 0-1 kHz range measured using a forceplate) in normal human walk is below 15 Hz [13]. The bandwidth of the input signals was set at 30 Hz, two times the maximum frequency of interest, and the experiment lasted 180 seconds after the first 5 seconds were removed. During the tests the subject was instructed to stand with one foot on the vibrating force plate while maintaining the contralateral foot on the walkway (Fig. 7). During this test, both DP and IE data were measured simultaneously. Since the perturbation platform applies disturbances to the ankle, the subject effectively tried to balance himself, generating uncorrelated torques with respect to the displacements resulting in poor coherence at low frequencies (bellow 3 Hz). A support frame (Fig. 7) was added so the subject could rely on its arms for balancing, greatly improving the coherence at low frequencies without affecting the impedance at higher frequencies. The impedance of the human ankle and force plate in both DP and IE were calculated using equations 6 and the impedance of the ankle was estimated by removing the force plate impedance as follows:

$$\mathbf{Z}|_{ankle} = \mathbf{Z}|_{ankle\ +\ force\ plate} - \mathbf{Z}|_{force\ plate} \qquad (8)$$

The ankle impedance during standing in both DP and IE can be seen in Fig. 8. The subject's quasi-static impedance magnitude (below 1 HZ) during standing was 50.08 dB (319 Nm/rad) in DP and 41.48 dB (119 Nm/rad) in IE. These values are larger than the ankle impedances reported no loading of the ankle which were reported at 25 dB in DP (18 Nm/rad) and 18 dB in IE (8 Nm/rad) [4] showing that the loading of the ankle has a substantial effect on its impedance.

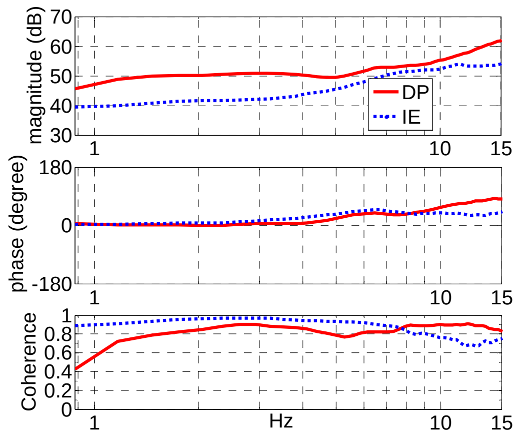

Fig. 8: Magnitude, phase, and coherence plots of the human subject's mechanical impedance in DP and IE.

CONCLUSION

This work presented the design and fabrication of a perturbation platform for estimation of the human ankle impedance during standing and walking in arbitrary directions without any wearable device. The platform was capable of generating torques similar to the human ankle. The force plate and camera system allowed for the estimation of the ankle torques and angles necessary for impedance estimation. Details of the fabrication of the device were presented, and the analytical tools required for the estimation of the ankle torques, angles, and impedances were discussed. A mockup with known stiffness was used to validate the capability of the system to estimate the impedance in two DOFs, which was shown to be within 5% of the expected value. A preliminary experiment with a human subject revealed that the quasi-static impedance of the human ankle during standing to be 50.08 dB (319 Nm/rad) in DP and 41.48 dB (119 Nm/rad) in IE.

FUTURE WORK

The main goal of developing the instrumented walkway was to estimate the mechanical impedance of the human ankle during walking in arbitrary directions. Future work will be focused on improving the design further and use it for the estimation of the ankle impedance during walking in different conditions, including straight walking, sidestep cutting, and different turning maneuvers. Additionally, ankle's impedance during walking on different ground profiles will be studies.

ACKNOWLEDGEMENT

This material is based upon work supported by the National Science Foundation under CAREER Grant No. 1350154.

REFERENCES

[1] Sup, F., 2009, "A Powered Self-Contained Knee and Ankle Prosthesis for near Normal Gait in Transfemoral Amputees," Ph.D. thesis, Vanderbilt University, Nashville, Tennessee.

[2] Eilenberg, M. F., Geyer, H., and Herr, H., 2010, "Control of a Powered Ankle–Foot Prosthesis Based on a Neuromuscular Model," IEEE Transactions on Neural Systems and Rehabilitation Engineering, 18(2), pp. 164-173.

[3] Hitt, J. K., Sugar, T. G., Holgate, M., and Bellman, R., 2010, "An Active Foot-Ankle Prosthesis with Biomechanical Energy Regeneration," J. Med. Devices, 4(1), pp.

[4] Rastgaar, M., Ho, P., Lee, H., Krebs, H. I., and Hogan, N., 2009, "Stochastic Estimation of Multi-Variable Human Ankle Mechanical Impedance," eds., Hollywood, CA, pp.

[5] Rastgaar, M., Ho, P., Lee, H., Krebs, H. I., and Hogan, N., 2010, "Stochastic Estimation of the Multi-Variable Mechanical Impedance of the Human Ankle with Active Muscles," eds., Boston, MA, pp.

[6] Lee, H., Ho, P., Krebs, H. I., and Hogan, N., 2009, "The Multi-Variable Torque-Displacement Relation at the Ankle," eds., Hollywood, CA, pp.

[7] Lee, H., Ho, P., Rastgaar, M., Krebs, H. I., and Hogan, N., 2010, "Quantitative Characterization of Steady-State Ankle Impedance with Muscle Activation," eds., Cambridge, MA, pp.

[8] Lee, H., Ho, P., Rastgaar, M., Krebs, H. I., and Hogan, N., 2011, "Multivariable Static Ankle Mechanical Impedance with Relaxed Muscles," Journal of Biomechanics, 44(pp. 1901-1908.

[9] Shamaei, K., Sawicki, G. S., and Dollar, A. M., 2013, "Estimation of Quasi-Stiffness and Propulsive Work of the Human Ankle in the Stance Phase of Walking," PLoS ONE, 8(3), pp. e59935.

[10] Rouse, E., Hargrove, L., Perreault, E., and Kuiken, T., 2012,

[11] H, L., and N, H., 2014, "Time-Varying Ankle Mechanical Impedance During Human Locomotion.," IEEE Trans Neural Syst Rehabil Eng., pp.

[12] Ficanha, E. M., Rastgaar, M., and Kaufman, K. R., in press, "Ankle Mechanics During Sidestep Cutting Implicates Need for 2-Degree of Freedom Powered Ankle-Foot Prosthesis," Journal of Rehabilitation Research and Development, 52(1), pp.

[13] Antonsson, E. K., and Mann, R. W., 1985, "The Frequency Content of Gait," Journal of Biomechanics, 18(1), pp. 8.

